EFFECT OF AN AXIAL HOLE ON NATURAL CONVECTION HEAT TRANSFER FROM A CYLINDRICAL PIN FIN ATTACHED TO A HORIZONTAL PLATE

by

Saurav MANNA[a], Subhas C. HALDAR[b,,**], and Subrata K. GHOSH[a]*

[a] Department of Mechanical Engineering, Indian School of Mines, Dhanbad, Jharkhand
[b] Department of Mechanical Engineering, Haldia Institute of Technology, West Bengal, India

Heat transfer under laminar natural convection from a hollow cylindrical fin mounted on a horizontal base plate has been numerically studied. The flow outside the fin is much stronger than that inside the hole and as a consequence the rate of heat transfer from a hollow fin is primarily due to the contribution by the outer surface of the fin. Fortunately, the rate of heat transfer is not negatively affected by the presence of the hole at the fin centre. On the contrary, when the Grashof number is higher or the hole diameter is bigger, the inside surface contributes marginally to the heat transfer. A hollow fin saves material and weighs less compared to a solid fin. So, this feature may be exploited.

Key words: *free convection, natural convection, pin fin, hollow fin, heat sink, thermal management, CFD*

Introduction

The incessant miniaturization of the electronic components increases the power density rendering the heat dissipation from the components a challenging task. This has sustained the research on the performances of different fin geometries of a heat sink. Usually a fan blows air over the heat sink used to cool a component having high power density and hence mixed convection is the mode of heat transfer. But for components with lower heat dissipation rate, heat sinks are cooled by free convection. Free convection should be given the first consideration for cooling since it is noise free and more reliable due to the absence of a fan and saves power.

Heat transfer from an array of fins depends on large number of parameters: geometry, length, thickness or diameter of the fins, spacing between them, the type of flow, and the thermal conductivity. Based on the cause of fluid flow, it is classified as free convection and forced convection. For cooling by free convection, rate of heat transfer additionally depends on the orientation of the fins. Forced flow again can be categorized as impinging or parallel to the base plate. Common fin geometries are either pin or plate types. Cross-section of the pins can be circular, square, or rectangular. Combinations of the variables mentioned above can produce large number of situations and considerable number of studies is required to cover these. This is another reason for large number of published articles on this topic. In order to be brief, only

---

2494

Manna, S., et al.: Effect of an Axial Hole on Natural Convection Heat Transfer ...
THERMAL SCIENCE: Year 2018, Vol. 22, No. 6A, pp. 2493-2502

some of the more recent papers dealing with mainly plate fins and pin fins of either circular or rectangular cross-section, the two most commonly used fin geometries will be discussed here.

A comparative study of heat sink having various fin geometry like a rectangular, a trapezoidal and an inverted trapezoidal under natural convection is investigated by Charles and Wang [1]. The test result revealed that heat transfer coefficient of the inverted trapezoidal fins is higher than the trapezoidal one by approximately 25% and rectangular fin by about 10%. Steady-state natural convection and radiation heat transfer from various shaped thin fin-arrays on a horizontal base plate has been numerically investigated by Dogan *et al.* [2].They have suggested an optimum fin shape that yields the highest average heat transfer coefficient. Huang *et al.* [3] have experimentally investigated the effect of orientation of square fins for free convective heat transfer performance. Test results show that the upward facing orientation yields the highest heat transfer coefficient compared to side and downward facing cases. It is also shown that the heat transfer coefficient initially increases with the finning factor, attains a maximum around 1.6-1.7, and then decreases. They also observed that the rate of heat transfer is maximum at a fin density of 1 pin/cm^2. Ahmadi *et al.* [4] have investigated the heat transfer characteristics of highly populated pin fin arrays for three different orientations in the gravity field. It is observed that among the three orientations, the vertically upward facing fin array yielded the highest heat transfer rates, followed by the horizontal fin array and the vertically downward facing fin array similar to the observation reported by Huang *et al.* [3]. They also specified the contribution of radiation heat transfer in combined mode of heat transfer and defined an optimal fin population. The effect of steady state external natural convective heat transfer of interrupted rectangular fins facing upward is investigated numerically and experimentally by Ahmadi *et al.* [4]. They concluded that adding interruptions to vertically-mounted rectangular fins can enhance the thermal performance considerably and that an optimum fin interruption exists. A correlation has been proposed for calculating the optimum interruption length. Tari *et al.* [5] have investigated the effect of natural convective heat transfer from a heat sink in both horizontal and slightly inclined from horizontal orientations. A set of Nusselt number correlations covering all possible angles is recommended.

Bhanja *et al.* [6] have studied numerically and analytically the temperature distribution and heat transfer rate from a porous pin fin subjected to natural convection. Zografos and Sunderland [7] have investigated heat transfer characteristics of three fin arrays. The fins are arranged inline and staggered under a variety of heat inputs and inclinations. The most significant outcome of this experiment is the optimum ratio of fin diameter to center-to-center spacing as 1/3. They also developed an empirical model that predicts the performance of pin fin arrays for a wide range of Rayleigh numbers and geometries. Experiments were carried out by Sparrow and Vemuri [8] to investigate the combined natural convection-radiation heat transfer characteristics of arrays having highly populated pin fins. It has been found that when the number of fins is increased with fixed values of the other parameters, the heat transfer increased at first, attained a maximum, and then decreased. In addition, results showed that the contribution of radiation was substantial and was greatest for more populous arrays, for longer fins, and at small temperature differences. Jang *et al.* [9] studied a radial heat sink with pin fins in order to obtain a lighter heat sink while maintaining a similar cooling performance to that of a plate-fin heat sink. It is found that the system is sensitive to the number of fins as well as the length of the fins. A design for the optimum radial heat sink has been proposed, which reduces the mass by more than 30% while maintaining a similar cooling performance to that of a plate-fin heat sink. A numerical analysis of laminar free convective heat transfer from a solid single pin fin attached to a horizontal base plate has been investigated by Haldar [10]. In this study a correlation is sug-

gested to predict the heat flux at the fin base for a given fin diameter to length ratio and Grashof number. This may be used to estimate the upper limit of free convection heat transfer from any horizontal heat sink with an array of circular pin elements. Radiation heat transfer from a pin fin array heat sink is studied theoretically and experimentally by Kobus and Oshio [11]. They introduced an effective radiation heat transfer coefficient that is added to convective heat transfer coefficient. Three dimensional laminar natural convective heat transfer of air filled rectangular enclosures with pin fins attached to the active wall has been studied numerically by Bocu and Altac [12]. This investigation reports the effects of various fin parameters such as number, length, orientation and diameter of the fins for the Rayleigh numbers ranging from 10^5 to 10^7. Elshafei [13] has experimentally studied the natural convective heat transfer from circular pin fin heat sinks. He performed experiments with heat sinks facing upward and sideward orientations with hollow and perforated fins. He observed that the solid pin fin heat sink performance for upward and sideward orientations shows a competitive nature, depending on Rayleigh number and generally shows higher heat transfer coefficients than those of the perforated/hollow pin fin ones in both arrangements. The notable limitation of the study was that the experiments were carried out within a very narrow range of Rayleigh number. The effect of rectangular fin dimensions on impingement heat transfer rate has been reported by Qiu *et al.* [14]. A review paper by Anandan and Ramalingam [15] discusses various techniques of electronic cooling as well as development of advanced materials and manufacturing methods.

The discussion on the literatures reveals that though there are large numbers of published articles on solid fins but very few on hollow fins. The article by Elshafei [13] is the only one on hollow pin fins the authors could locate and this deals with a very narrow range of Rayleigh numbers from $3.8 \cdot 10^6$ to $1.65 \cdot 10^7$. This gap in the literature provided the motivation to carry out this research. In the present study, free convective heat transfer about a hollow circular pin fin attached to a horizontal base plate has been investigated numerically. Heat transfer performance of the hollow fin is then compared to the solid one having the same dimensions.

Problem description

Figure 1 presents the schematic of the problem along with the chosen co-ordinate system and the respective velocity components. The direction of gravity in the figure is vertically downward. A hollow fin of circular cross-section having diameters D_i and D_o, and length L is attached to a horizontal base plate. The angular symmetry about the fin axis makes it a 2-D problem. The base of the fin and the portion of the base plate within the hollow fin ($r \leq D_o/2$) were considered isothermal. While the rest of the base plate was assumed adiabatic in order to study the contribution to heat transfer by the fin alone.

Governing equations and boundary conditions

The computational domain, marked in fig. 1, includes the fin as well as the fluid surrounding the fin.

For the fin, solid or hollow, only the conduction equation in (r, z) co-ordinates needs to be considered. Equation (1) is the dimensionless form:
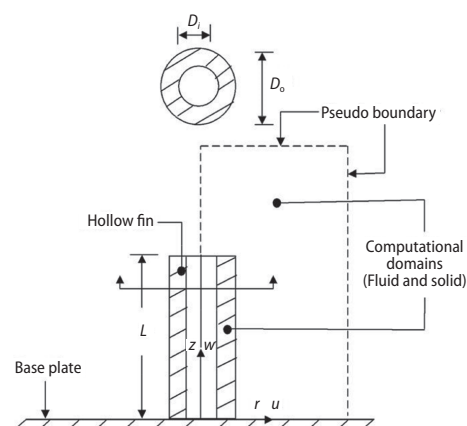

Figure 1. Schematic of the physical problem and the computational domain

$$\frac{\partial^2 t}{\partial r^2} + \frac{1}{r}\frac{\partial t}{\partial r} + \frac{\partial^2 t}{\partial z^2} = 0 \tag{1}$$

Thermal boundary conditions to solve eq. (1) are discussed:

$$t = 1.0 \quad \text{at the fin base, } i.\, e. \quad r_i \le r \le r_o \quad \text{at} \quad z = 0 \tag{1a}$$

$$k_{\text{fin}}\frac{\partial t}{\partial r}\bigg|_{\text{fin}} = k_{\text{fluid}}\frac{\partial t}{\partial r}\bigg|_{\text{fluid}} \quad \text{at the inner and outer vertical surfaces of the fin} \tag{1b}$$

$$k_{\text{fin}}\frac{\partial t}{\partial z}\bigg|_{\text{fin}} = k_{\text{fluid}}\frac{\partial t}{\partial z}\bigg|_{\text{fluid}} \quad \text{at the fin tip, and} \tag{1c}$$

$$\frac{\partial t}{\partial r} = 0 \quad \text{at the central axis of the fin} \tag{1d}$$

For the case of solid fin, there is no inner surface and eq. (1b) is applicable only at the outer surface.

For the fluid surrounding the fin, conservation of mass, energy, and radial and axial components of momentum constitute the governing equations. The cross differentiation of the two components of the momentum equations helps to recast the equations in terms of azimuthal vorticity and steam-function. Boussinesq's approximation has been applied to the buoyancy term. The definition of stream-function automatically satisfies the conservation of mass. The governing equations are then made dimensionless. All the symbols have been defined in the no-menclature. The dimensionless variables have been defined alongside their dimensional counterparts. The set of governing equations in dimensionless form are:

$$u\frac{\partial \Omega}{\partial r} + w\frac{\partial \Omega}{\partial z} = \left(\frac{\partial^2 \Omega}{\partial r^2} + \frac{1}{r}\frac{\partial \Omega}{\partial r} + \frac{\partial^2 \Omega}{\partial z^2} - \frac{\Omega}{r^2}\right) - \text{Gr}\frac{\partial t}{\partial r} \tag{2}$$

$$-\Omega r = \frac{\partial^2 \psi}{\partial r^2} - \frac{1}{r}\frac{\partial \psi}{\partial r} + \frac{\partial^2 \psi}{\partial z^2} \tag{3}$$

$$u\frac{\partial t}{\partial r} + w\frac{\partial t}{\partial z} = \frac{1}{\text{Pr}}\left(\frac{\partial^2 t}{\partial r^2} + \frac{1}{r}\frac{\partial t}{\partial r} + \frac{\partial^2 t}{\partial z^2}\right) \tag{4}$$

The stream-function and the two velocity components are related:

$$u = -\frac{1}{r}\frac{\partial \psi}{\partial z} \quad \text{and} \quad w = \frac{1}{r}\frac{\partial \psi}{\partial r} \tag{5}$$

To carry out the numerical computation, two imaginary boundaries, one horizontal and one vertical, were considered as shown in fig. 1. Locations of both these boundaries should be far enough from the fin so that they do not influence the results of the numerical solution. It is a common practice to assume that the fluid crosses these far-off boundary surfaces orthogo-nally. The boundary conditions for the fluid region are then specified.
– Base plate inside a hollow fin:

$$t = 1.0 \quad \text{for} \quad r \le r_i \quad \text{at} \quad z = 0$$

- Vertical fin surfaces: since it is a solid surface, $\psi = 0$ at all values of z on this surface. As a result, $\partial^2\psi/\partial z^2 = 0$. Also, $(1/r)(\partial\psi/\partial r) = w = 0$ due to no slip, and eq. (3) reduces to $\Omega = -(1/r)(\partial^2\psi/\partial r^2)$. Temperature boundary condition on these surfaces has been stated in eq. (1b).
- Fin tip: because it is a solid surface, $\psi = 0$ at all values of r on this boundary. This yields $\partial^2\psi/\partial r^2 = \partial\psi/\partial r = 0$. Equation (3) then becomes $\Omega = -(1/r)(\partial^2\psi/\partial z^2)$. Equation (1c) provides the thermal boundary condition.
- Base plate outside the fin: $\psi = 0$ and eq. (3) reduces to $\Omega = -(1/r)(\partial^2\psi/\partial z^2)$. This part of the base plate was assumed adiabatic in order to study the performance of the fin alone and accordingly $\partial t/\partial z = 0$.
- Vertical pseudo boundary: The assumption of orthogonal flow across this boundary yields $\partial\psi/\partial r = \partial^2\psi/\partial r^2 = 0$ and also $\partial\Omega/\partial r = 0$. Fluid enters the computational domain at the free stream temperature and hence $t = 0$ if $u < 0$ on this boundary. If the fluid leaves through this boundary, identified by $u > 0$, then $\partial t/\partial r = 0$.
- Horizontal pseudo boundary: orthogonal flow across this boundary yields $\partial\psi/\partial z = \partial^2\psi/\partial z^2 = 0$ and $\partial\Omega/\partial z = 0$. Thermal conditions on this boundary are $\partial t/\partial z = 0$ if $w > 0$ (outflow) and $t = 0$ if $w < 0$ (inflow).
- Fin centre line: symmetry about the centre line dictates $\partial\psi/\partial r = \partial t/\partial r = 0$ as well as $\Omega = 0$.

Numerical method

The numerical code for this investigation was developed by the authors. The eqs. (2) and (4) were recast in conservative form and then solved along with the other equations by finite difference technique. The equations were discretized by dividing the computational domain with non-staggered control volumes following the cell average QUICK scheme proposed by Leonard [16]. According to Sharma and Eswaran [17], QUICK scheme is expected to yield grid-independent results with fewer grids in comparison to second order upwinding. The wall adjacent control volumes were discretized by central difference technique.

To initiate the numerical solution, the dimensionless temperatures everywhere within the computational domain were specified as zero except at the base of the fin where the temperature was unity as per the chosen boundary condition. Solution of eq. (1) provided the temperature distributions within the fin which were then used in the discretized form of eqs. (1b), (1c), and (1d) to update the temperature values at the fin boundaries. In the fluid region, eq. (4) was solved for t, eq. (2) for Ω, eq. (3) for ψ, and eq. (5) for velocities u and w from ψ. Vorticity values at the fluid boundary were then updated satisfying the corresponding vorticity boundary condition stated before and this solution of eqs. (1)-(5) constitutes one iteration cycle. The cycle was repeated utill the desired convergence was accomplished.

Each individual equation was iterated up to a convergence of 0.0001%. The cycle of iteration was continued till the differences of vorticity values at each grid point between two consecutive iteration cycles were less than 0.001%.

In order to determine suitable grid spacing for grid-independent results, the code was run with various pairs of radial and axial grid spacing. The spacing along one co-ordinate direction was gradually reduced keeping the spacing along the other co-ordinate fixed. This yielded a uniform radial spacing of 0.01 and a uniform axial spacing of 0.01 as acceptable for the fluid region while the solid fin was discretized by choosing an axial spacing of 0.01 and 20 divisions along the radial direction.

A study was next performed to establish suitable locations of the two imaginary boundaries. The code was run to generate results by moving one of the two pseudo boundaries

2498

Manna, S., *et al.*: Effect of an Axial Hole on Natural Convection Heat Transfer ...
THERMAL SCIENCE: Year 2018, Vol. 22, No. 6A, pp. 2493-2502

at a time while keeping the other at a fixed place. Expectedly, as the distance of these boundaries from the fin increases, their effects on the results were found to fade away gradually. The vertical boundary at a radial distance of 1.0 and the horizontal boundary at an axial distance of 1.2 were accepted. If these boundaries are located farther away from the fin, it will increase the size of the computation domain without significant improvement in results.

The rate of heat transfer from the fin can be determined by three means; from conduction across the fin base, from convection at the fin surfaces in contact with the fluid, and lastly from the heat carried away by the fluid. Heat transfer values obtained by all the three methods are supposed to be equal. Accordingly, these three values obtained from numerical solution were used to check the accuracy of the code.

Results and discussions

Results were generated for Gr based on fin length within the range of 10^2 to 10^6, fin outer diameter to length ratio of 0.1 to 0.5 and ratio of inner to outer diameter of the fin 0 to 0.8. The fin to fluid thermal conductivity ratio was selected as 10000 which approximates the thermal conductivity of aluminum alloys, the material most commonly used for heat sinks, to that of air. Air was selected as the fluid enveloping the fin by specifying a Pr value of 0.7 in eq. (4). It may be stated here that the case of $D_i/D_o = 0$ corresponds to a solid fin. A fin length of 40 mm and a plate temperature of 50 °C above ambient yield a Gr value of about 2×10^5 for which the flow is laminar. So, the range selected for Gr (10^2 to 10^6) cover most practical applications.

In order to observe the flow pattern, the velocity vectors have been presented in fig. 2 for the case of $D_o/L = 0.5$, $D_i/D_o = 0.8$ and for three Gr values. Velocity values inside the hole are quite smaller than those outside the fin and this compelled to plot them separately. At a Gr value of 10^2, the fluid inside the fin hole is almost stagnant as seen in fig. 2(a). As Gr increases, the flow becomes stronger and is able to gradually penetrate the fin hole, figs. 2(b) and 2(c). The higher velocity values near the hole centre compared to those at the hole periphery in fig. 2(c) are dictated by the mass conservation since the flow area increases with the increase in distance from the centre.

Outside the fin, the fluid enters through the vertical boundary horizontally which then gradually turns upwards as it approaches the fin and becomes almost vertical near the fin boundary, figs. 2(d) and 2(e). Finally, the fluid leaves through the horizontal pseudo boundary at the top of the fin. At higher Gr, fluid is also drawn through central part of the top horizontal boundary which then moves downwards to the hole of the fin, fig. 2(e).

The rate of heat transfer from a solid fin will be taken as a reference and hence it will be discussed first. Figure 3 presents the dimensionless rate of heat transfer from solid fins as a function of fin outer diameter to length ratio for various Gr values. As fin diameter to length ratio approaches zero implying the condition of no fin, the rate of heat transfer also approaches zero for each of the profiles. At a given diameter to length ratio, rate of heat transfer grows with Gr as expected. As the diameter to length ratio increases, the fin becomes thicker and as expected the rate of heat transfer increases at a particular Gr value. But this increase in heat transfer comes at the expense of the fin occupying more base area.

For hollow fins, the inner cylindrical surface provides an additional area contributing to the heat transfer apart from the outer cylindrical surface and the tip of the fin. The total rate of heat transfer consists of contributions by these three surfaces. The figs. 4(a) and 4(b) plot the rate of heat transfer with Gr for a fixed value of hole diameter to fin outer diameter ratio for two different values of fin outer diameter to length ratio. For the slender fin with $D_o/L = 0.2$, fig. 4(a), the contribution to heat transfer by the inside surface is negligible. This is because the fluid inside
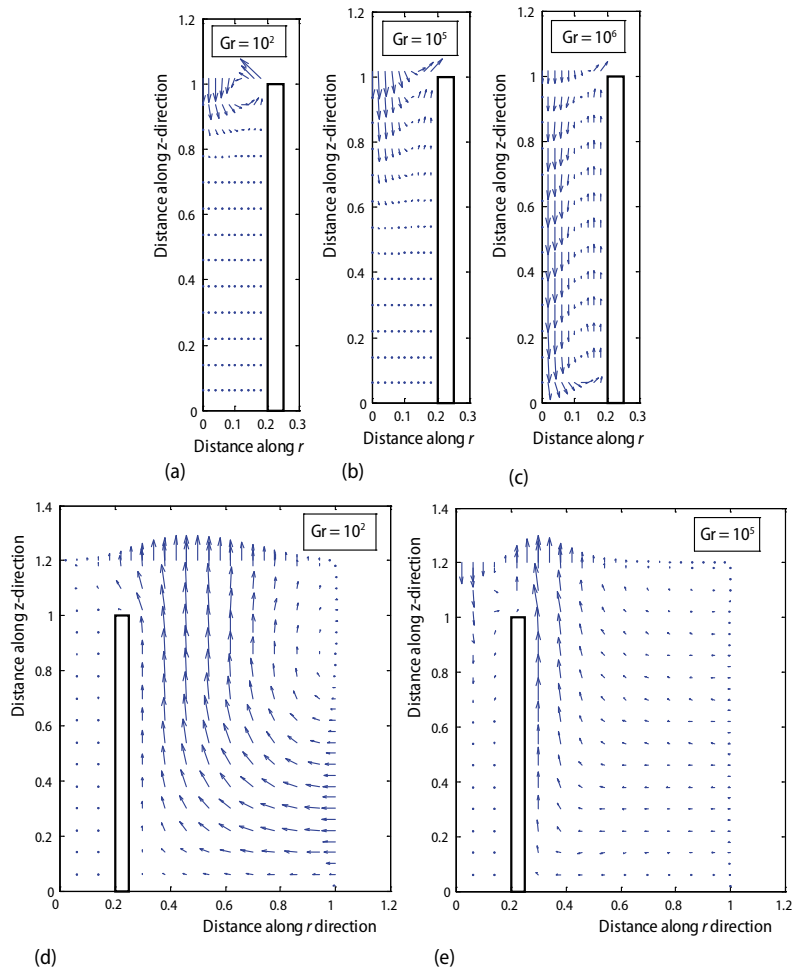
Manna, S., *et al.*: Effect of an Axial Hole on Natural Convection Heat Transfer ...
THERMAL SCIENCE: Year 2018, Vol. 22, No. 6A, pp. 2493-2502

2499

Figure 2. Velocity vectors for $D_o/L = 0.5$ and $D_i/D_o = 0.8$

the hole remains almost stagnant as discussed before and the heat transfer is primarily from the outside surface of the fin. For a thicker fin, fig. 4(b), the contribution by the inside surface increas-

es with Gr though the contribution to total heat transfer is extremely small. It may be mentioned here that the results reported by Elshafei [13] also reveal little influence of hole size on heat transfer and this corroborates our results.

The contribution to heat transfer by the tip of the fin is very little and can be obtained by subtracting the contributions by the inside and outside surfaces from the total. The profiles for the tip have not been included for the clarity of the figures.

If the hole is made bigger as reflected by a higher value of D_i/D_o, the contribution to
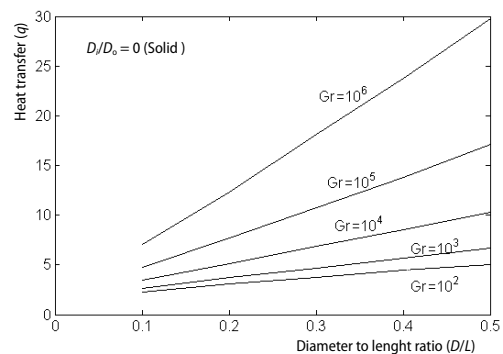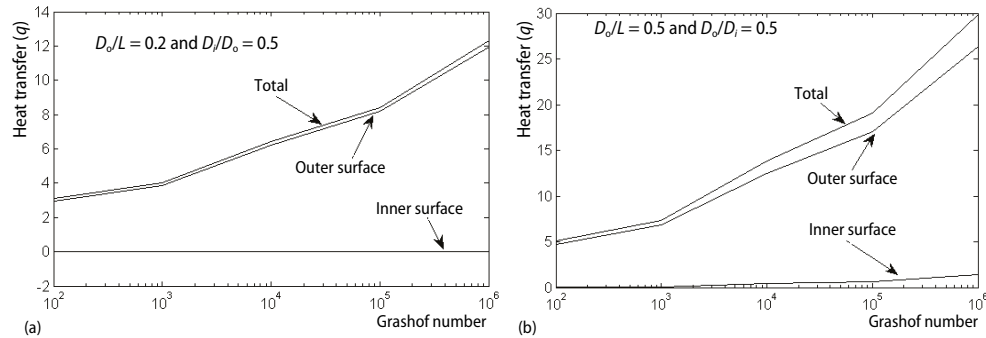

Figure 3. Heat transfer from solid fins

2500

Manna, S., *et al.*: Effect of an Axial Hole on Natural Convection Heat Transfer ...
THERMAL SCIENCE: Year 2018, Vol. 22, No. 6A, pp. 2493-2502

Figure 4. Contribution to heat transfer by inside and outside fin surfaces
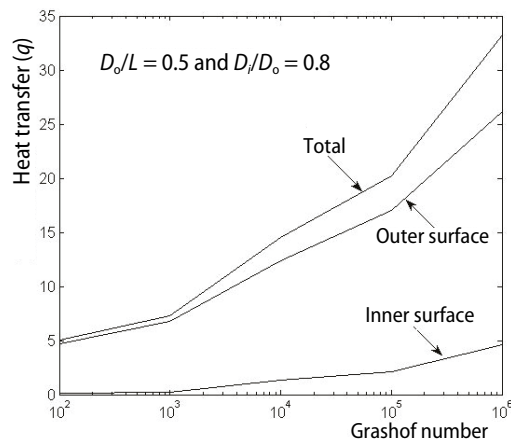
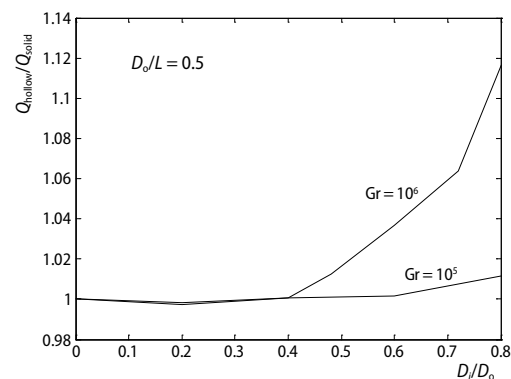**Figure 5. Heat transfer from a fin with bigger hole**

Figure 6. Effect of hole size on heat transfer

heat transfer by the inner surface marginally increases, fig. 5. This is due to the fact that increase in hole size facilitates fluid motion inside the hole.

The primary focus of this study is to investigate the influence of the hole on rate of heat transfer from the fin. Accordingly, ratio of heat transfer from a hollow fin to a solid fin of same diameter and length has been plotted against hole size in fig. 6. Up to a D_i/D_o value of 0.4, the hole has almost no effect on the rate of heat transfer. This is due to the fact that the hole size is too small for the fluid inside to have any convective motion. At a Gr value of 10^6, the contribution to the heat transfer by the hole increases with the increase in hole diameter beyond a D_i/D_o value of 0.4 for the case of D_o/L equals to 0.5.

According to the results presented above, if a hole is made at the fin centre the rate of heat transfer remains nearly the same as that of the solid fin without the hole for most of the practical operating regions. But a hollow fin offers other advantages over the solid fin. It requires less material and consequently saves money as well as weight.

Conclusions

Laminar free convection about a cylindrical fin having an axial hole at its centre and attached to a horizontal circular base plate has been investigated numerically. The primary purpose of this study is to investigate the influence of the hole on rate of heat transfer by the fin. Heat transfer by a hollow fin to the surrounding air takes place from outer cylindrical surface, inner cylindrical surface and tip of the fin. At lower Grashof numbers, the flow is not strong

Manna, S., *et al.*: Effect of an Axial Hole on Natural Convection Heat Transfer ...
THERMAL SCIENCE: Year 2018, Vol. 22, No. 6A, pp. 2493-2502

2501

enough to penetrate the hole and the fluid remains almost stagnant inside the hole. As a consequence, the contribution to heat transfer by the hole is negligible. With increase in Grashof number or the hole size, the fluid inside the hole is able to move and marginally contributes to the rate of heat transfer. Though the axial hole has little contribution to heat transfer but it has other merits over a solid fin. The holes save material and reduce the weight of the heatsink. So, a heatsink with hollow fins is benefitted from these advantages without degrading its thermal performance.

Nomenclature

D_i – hole diameter, [m]
D_o – outer diameter of the fin, [m]
Gr – Grashof number, $[= g\beta(T_b - T_o)L^3/\vartheta^2]$, [–]
g – acceleration due to gravity, [ms^{-2}]
k_{fin} – thermal conductivity of fin, [Wm^{-1}K^{-1}]
k_{fluid} – thermal conductivity of fluid, [Wm^{-1}K^{-1}]
L – length of the fin, [m]
Pr – Prandtl number (= ϑ/α), [–]
Q – rate of heat transfer,
    $\{q = Q/[k_{fluid}(T_b - T_o)L]\}$, [W]
R – radial co-ordinate, ($r = R/L$), [m]
T – temperature, $[t = (T - T_o)/(T_b - T_o)]$, [K]
T_b – base temperature, (t_b = 1.0), [K]

T_o – free stream temperature, (t_o= 0), [K]
U – velocity along R, $[u = U/(\vartheta/L)]$, [ms^{-1}]
W – axial velocity, $[w = W/(\vartheta/L)]$, [ms^{-1}]
Z – -axial co-ordinate, ($z = Z/L$), [m]

Greek symbols

α – thermal diffusivity, [m^{2}s^{-1}]
β – volumetric coefficient of thermal
    expansion, [K^{-1}]
ϑ – kinematic viscosity, [m^{2}s^{-1}]
σ – vorticity about Z, $[\Omega = \sigma/(\vartheta/L^2)]$, [s^{-1}]
Ψ – stream-function, ($\psi = \Psi/\vartheta$), [m^{2}s^{-1}]

References

[1] Charles, R., Wang, C. C., A Novel Heat Dissipation Fin Design Applicable for Natural Convection Augmentation, *International Communications in Heat and Mass Transfer, 59* (2014), Dec., pp. 24-29

[2] Dogan, M., *et al*., Numerical Analysis of Natural Convection and Radiation Heat Transfer from Various Shaped Thin Fin-Arrays Placed on a Horizontal Plate – A Conjugate Analysis, *Energy Conversion and Management, 77* (2014), 1, pp. 78-88

[3] Huang, R. T., *et al*., Natural Convection Heat Transfer from Square Pin Fin Heat Sinks Subject to the Influence of Orientation, *Proceedings*, Semiconductor Thermal Measurement and Management Symposium, 2006 IEEE Twenty-Second Annual IEEE, Dallas, Tex., USA,

[4] Ahmadi, M., *et al*., Natural Convection from Rectangular Interrupted Fins, *International Journal of Thermal Sciences, 82* (2014), Aug., pp. 62-71

[5] Tari, I., Mehrtash, M., Natural Convection Heat Transfer from Horizontal and Slightly Inclined Plate-Fin Heat Sinks, *Applied Thermal Engineering, 61* (2013), 2, pp. 728-736

[6] Bhanja, D., *et al*., Thermal Analysis of Porous Pin Fin Used for Electronic Cooling, *Procedia Engineering, 64* (2013), Dec., pp. 956-965

[7] Zografos, A. I., Sunderland, J. E., Natural Convection from Pin Fin Arrays, *Experimental Thermal and Fluid Science, 3* (1990), 4, pp. 440-444

[8] Sparrow, E. M., Vemuri, S. B., Natural Convection/Radiation Heat Transfer From Highly Populated Pin Fin Arrays, *J. Heat Transfer, 107* (1985), 1, pp. 190-197

[9] Jang, D., *et al*., Multidisciplinary Optimization of a Pin-Fin Radial Heat Sink for LED Lighting Applications, *International Journal of Heat and Mass Transfer, 55* (2012), 4, pp. 515-521

[10] Haldar, S. C., Natural Convection about a Cylindrical Pin Element on a Horizontal Plate, *International Journal of Thermal Science, 49* (2010), Oct., pp. 1977-1983

[11] Kobus, C. J., Oshio, T., Predicting the Thermal Performance Characteristics of Staggered Vertical Pin Fin Array Heat Sinks under Combined Mode Radiation and Mixed Convection with Impinging Flow, *International Journal of Heat and Mass Transfer, 48* (2005), Mar., pp. 2684-2696

[12] Bocu, Z., Altac, Z., Laminar Natural Convection Heat Transfer and Air Flow in Three-Dimensional Rectangular Enclosures with Pin Arrays Attached to Hot Wall, *Applied Thermal Engineering, 31* (2011), 16, pp. 3189-3195

[13] Elshafei, E. A. M., Natural Convection Heat Transfer from a Heat Sink with Hollow/Perforated Circular Pin Fins, *Energy, 35* (2010), 7, pp. 2870-2877

[14] Qiu, S., *et al.*, Enhanced Heat Transfer Characteristics of Conjugated Air Jet Impingement on a Finned Heat Sink, *Thermal Science, 21* (2017), 1A, pp. 279-288

[15] Anandan, S. S., Ramalingam, V., Thermal Management of Electronics: A Review of Literature, *Thermal Science, 12* (2008), 2, pp. 5-26

[16] Leonard, B. P., Bounded Higher-Order Upwind Multidimensional Finite-Volume Convection-Diffusion Algorithms, in: *Adv. in Num. Heat Transfer* (Eds. W. J. Minkowycz, E. M. Sparrow), Vol.1, Taylor and Francis, New York, USA, 2000

[17] Sharma, A., Eswaran, V., Conservative and Consistent Implementation and Systematic Comparison of SOU and QUICK Schemes for Recirculating Flow Computation on a Non-Staggered Grid, *Proceedings*, 2nd Int. and 29th National FMEP Conf., Roorkee, India, 2002, pp. 351-358